Deep-UV Raman Scattering Analysis of Re-Crystallization in Ultra-Shallow Junction Implanted Si under Various Annealing Conditions

Takashi Sasaki[1*], Shintaro Nishibe[1], Hiroaki Minami[1]
Kenji Kisoda[2], Toshiyuki Isshiki[1], Masahiro Yoshimoto[1], Woo Sik Yoo[3] and Hiroshi Harima[1]

[1]Kyoto Institute of Technology
Matsugasaki, Kyoto 606-8585, Japan
Phone: +81-75-724-7421 [*]E-mail: dj020047@djedu.kit.ac.jp
[2]Wakayama University
Wakayama 640-8510, Japan
[3]WaferMasters, Inc.
San Jose, California, 95112, U.S.A.

1. Introduction

Formation of ultra shallow junctions is a key issue for further miniaturization of integrated circuits. For that purpose, ion-implantation of dopants in a very thin, 10nm layer in Si substrates has been extremely challenging. The ion-implantation should be combined with a novel thermal annealing technique to activate the dopants and to recover the crystal quality of the implanted region without significant diffusion of the dopant species.

Obviously, a quick and nondestructive characterization technique for such surface regions is very convenient in optimizing the process conditions. From this viewpoint, Raman spectroscopy using UV lasers for excitation is very promising. This is due to the shallow penetration depth of UV radiation in Si. For example, UV lasers with wavelength λ_{ex}=266 and 364 nm have absorption coefficients in Si of α =2.03 x10^6 and 9.95x10^5 cm^{-1}, respectively. Using backscattering geometry for the detection of scattered light, we find, by simple algebra, considering absorption of the incident and scattered light, about 90% of the backscattered signal is derived from the top surface region with depth δ =1/α~5 nm and ~10 nm, respectively. Thus, we may regard δ as an effective penetration depth in Raman scattering. We have previously shown that the re-crystallization process for B-implanted layers in Si within ~10 nm from the surface is successfully characterized by UV-Raman scattering. Good correlation between the results of Raman scattering and high-resolution cross-sectional transmission electron microscopy (HRTEM) has been obtained [1].

Here, we will use UV-Raman spectroscopy to evaluate shallow-implanted regions with B, As and P ions in Si, and compare the annealing effects between a flash lamp and an electric hot plate system.

2. Experiment

The experimental method is illustrated in the flow chart shown in Fig. 1. Ion-implanted Si wafers are annealed using two annealing techniques at different power or temperatures. The annealed samples are measured (sheet resistance) for activation and analyzed using UV-Raman spectroscopy. Subsequently they are analyzed for junction depth using Secondary Ion Mass Spectrometry (SIMS) and for visual characteristics using Transmission Electron Microscopy (TEM). The SIMS and TEM analyses are not part of this experimental work.

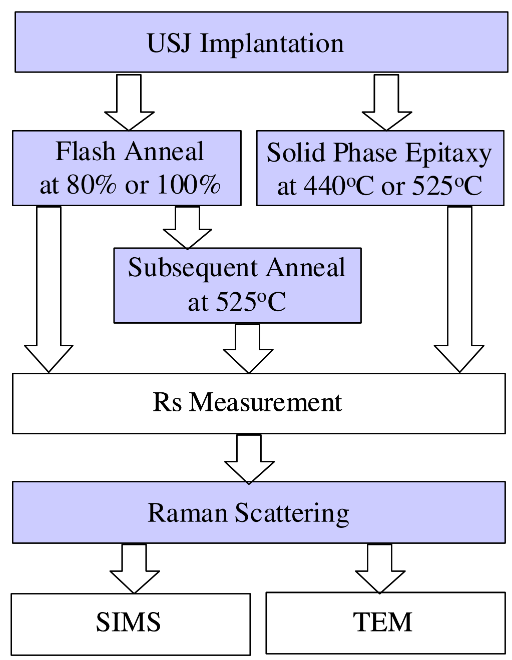

Fig. 1. Flow chart of the experimental method of this study.

3. Sample preparation

B, As and P ions were separately implanted on p-type Si (100) wafers at acceleration voltage of 1 keV (B, P) or 2 keV (As). For B-implantation, two types of wafers were prepared; one pre-amorphized by Ge-ion implantation to 5 x10^{15} cm^2 at 5 keV, and the other without pre-amorphization. The projected range of dopants was designed to be less than 10 nm for all cases.

The implanted wafers were annealed using a flash-lamp annealing system, WaferMasters' FLA-300 [2 - 6], or an electric hot plate system [6] for solid phase epitaxy (SPE). In the former system, the wafers were kept at 440°C and irradiated by a Xe-arc flash lamp with ~1 ms flash duration. The total power of the flash was about 0.5 MJ (called here as 100% flash) or 0.4 MJ (80% flash). In the latter system, the hot plate was set at either 440°C or 525°C and the annealing was done for 5 min.

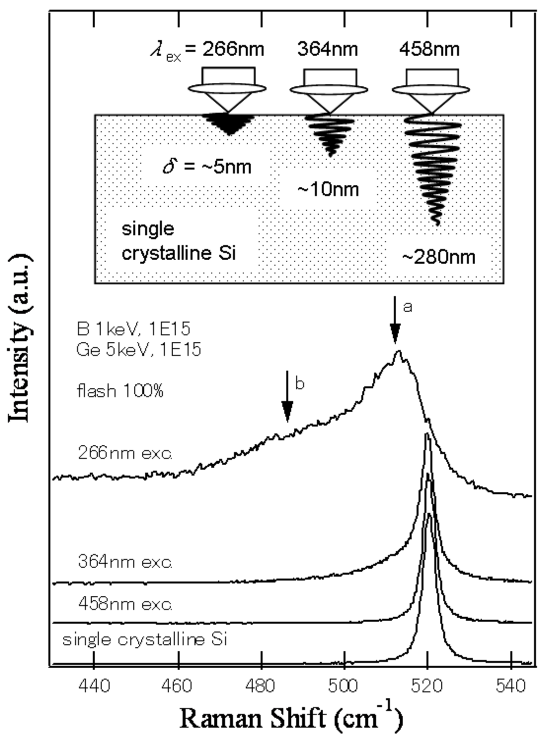

Fig. 2. Raman spectra of B-implanted Si wafer after flash annealing. The wafer was pre-amorphized by Ge-implantation. Lasers with different penetration depths (see inset) were tested.

4. Results

First, shallow penetration depth of UV radiation was confirmed by Raman observation of the implanted region of an annealed sample using different laser frequencies or penetration depths δ. In Fig. 2, Raman spectra of the B-implanted wafer with pre-amorphization after 100% flash-lamp annealing are plotted and compared with that of a virgin Si wafer (bottom). The virgin wafer gives a sharp phonon peak at 520.3 cm^{-1} with FWHM~3 cm^{-1}. A visible laser with λ_{ex}=458 nm, δ~280 nm (see the inset illustration in Fig. 2), which was also tested for comparison, gives almost the same sharp phonon peak as that of virgin Si. If λ_{ex}=364 nm (δ~10 nm) is employed, the main peak is slightly broadened and skewed to lower frequency. If λ_{ex}=266 nm (δ~5 nm) is employed, the spectrum gives a completely different feature: it consists of a broad signal peaked at ~515 cm^{-1} (arrow a) with a shoulder at ~480 cm^{-1} (arrow b). As shown in Fig. 3, the spectrum for λ_{ex}=266 nm is resolved into two main components, polycrystalline (disordered) Si (I_{poly}) and amorphous Si (I_a). Such a two-phase structure has been commonly observed in ion-implanted Si [7] or thin Si films grown by chemical vapor deposition [8]. The peak frequency and width of the I_{poly} signal is a good measure of the defect-free dimension L in Si (a measure of short-range order) [7]. Here we can estimate L~2-5 nm. Since no signals from the un-implanted (or un-damaged) region are included in the spectra, the implanted region is assumed to cover the penetration depth δ~5 nm. In contrast,, for λ_{ex}=458 nm, weak signals from the implanted region are overwhelmed by the strong signal from the Si crystal under the implanted region. The result for λ_{ex}=364 nm corresponds to a middle case: its tail is derived from a polycrystalline Si layer in the implanted region. These results suggest that a sharp transition occurs in this sample from a heavily implanted (or damaged) region to an un-implanted (or undamaged) region at depth ~5 nm from the surface.

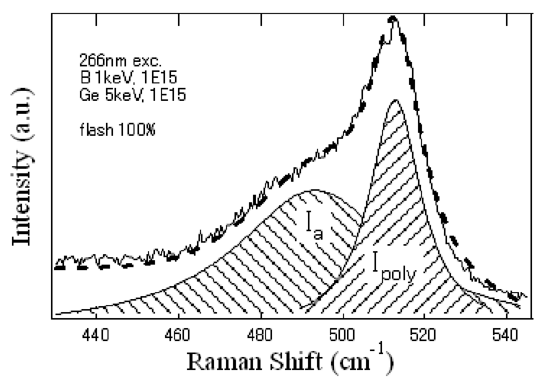

Fig. 3 Resolution of Raman spectrum for B-implanted wafer after flash annealing.

Next, we compared the effect of annealing using either the flash-lamp system or the thermal (hot-plate) system. Figure 4 plots Raman spectra observed at λ_{ex}=266 nm for the B-implanted wafers with pre-amorphization, showing (from top to bottom) as-implanted, hot-plate annealed (SPE) at 440°C and 525°C, and lamp-annealed wafers at 80% and 100% flash. The as-implanted sample is completely dominated by the amorphous Si signal. However, a very weak crystal Si signal also appears at 520 cm^{-1}, which indicates that there is a sharp interface between the amorphized and undamaged region near the probed depth δ ~5 nm. The SPE annealing at 440°C causes no significant change in crystal quality. However, SPE at 525°C clearly reduces the amorphous component and induces disordered recrystallization as suggested by the broadening and tailing of the crystalline Si signal. The lamp annealing, both 80% and 100% flash power, promotes these changes much more efficiently. We find, by closer inspection of the spectra, that the 100% flash presents a sharper polycrystal-like (disordered) Si peak (see arrow) located at higher frequency than that of the 80% flash. These results suggest that the degree of crystal quality in the recrystallized layer increases with increasing flash-lamp energy.

Finally, the annealing effect was compared for different dopant species. Ion-implanted wafers without the pre-amorphization process were observed. Figure 5 (a) plots Raman spectra at λ_{ex}=266 nm for the as-implanted samples with As, P and B, and Fig. 5 (b) shows the corresponding Raman spectra after the 100% flash-lamp annealing. Figure 5 (a) shows that the amorphous Si component at ~480 cm^{-1} becomes larger in order from B to P to As. This suggests that the lattice damage increases with the mass of the dopant species. The polycrystal-like (disordered) Si peak has almost the same spectral line shape for different dopants, but shows a systematic reduced frequency shift from B to As. This is probably due to lattice expansion induced by implantation [9]. This effect increases with the ionic radius of the dopant. We find in Fig. 5(b) that the amorphous component is reduced by the flash-lamp annealing for As and P. However, the recrystallization process is much less efficient when compared to the result for pre-amorphized wafers (compare with the significant change shown in Fig. 4, from the top to the bottom spectrum). Inefficient recovery of crystal quality by annealing without the pre-amorphization process is most evident in B-doping: The traces in Figs.5 (a) and (b) show that the amorphous component did not decrease by annealing, or maybe slightly increased. This is a puzzling result that needs further investigation. Comparison between the wafers with and without the pre-amorphization process (Figs. 4 and 5) suggests that thermal recrystallization depends on the degree of amorphization in as-implanted wafers.

The curve for B implanted wafers in Fig. 5 shows interesting behavior which we note here. The peak appears shifted and broadened while the contribution of the amorphous signal appears unchanged. The interpretation of this will be left for a future study.

5. Conclusions

By deep-UV Raman scattering, we have characterized the recrystallization process of Si wafers that were ion-implanted with As, P and B in a very thin top layer. Thermal annealing was conducted in two ways; flash-lamp annealing and thermal annealing (hot plate). Our results suggested that the recrystallization process occurred more efficiently by flash-lamp annealing. Furthermore, a pre-amorphization of a wafer by Ge-implantation prior to the main implantation process was very effective in promoting the recrystallization process.

It will be of great interest, to directly observe the evolution of crystal-lattice recovery by high-resolution cross-sectional transmission electron microscopy (TEM).

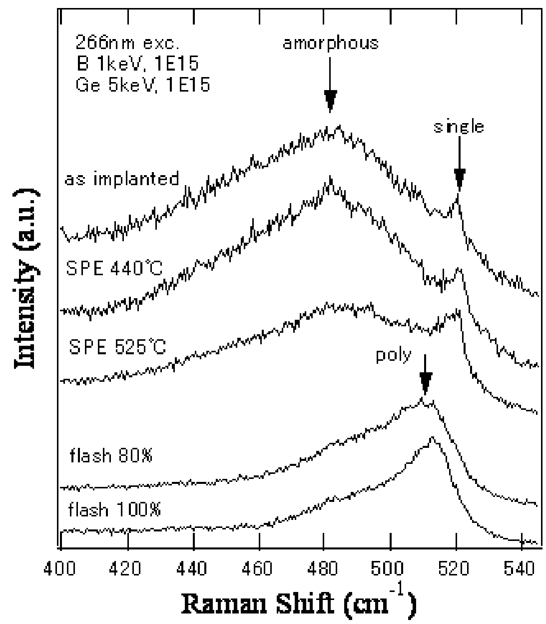

Fig. 4 Raman spectra of B-implanted wafer after flash and hot plate (SPE) annealing.

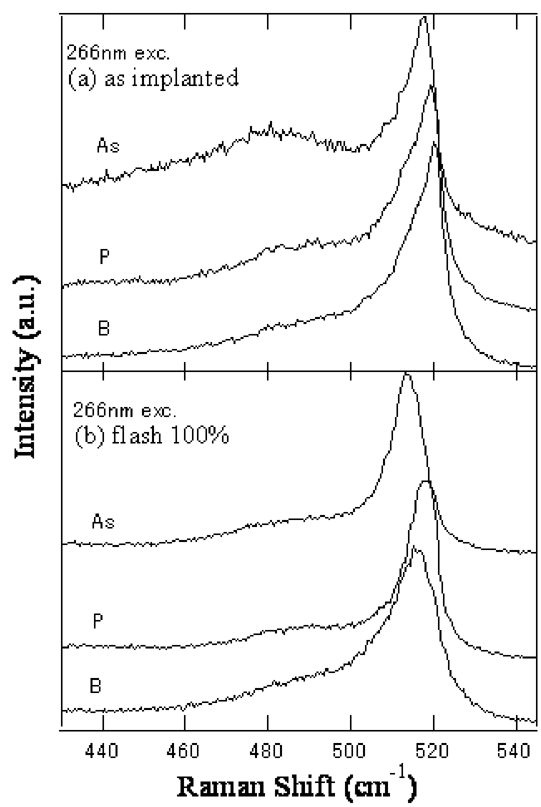

Fig. 5 Raman spectra of as-implanted wafers (a) and flash-lamp annealed (b).

References

[1] M.Yoshimoto, H.Nishigaki, H.Harima, T.Isshiki, K.Kang and W.S.Yoo, *J.Electrochem.Soc.* **153** G679 (2006)

[2] W.S. Yoo and K. Kang, *Electrochem. Soc. Proc.,* **PV 2003-14** 111 (2003).

[3] W.S. Yoo and K. Kang, *Electrochem. Soc. Proc.,* **PV 2004-1** 3 (2004).

[4] W.S. Yoo, US Patent 6.376,806.

[5] W.S. Yoo, US Patent 6,911,376.

[6] W.S. Yoo, US Patent 6,809,035.

[7] X.Huang, F.Ninio, L.J.Brown and S.Prawer, *J.Appl.Phys.* **77** 5910 (1995).

[8] R.Tsu, J.Gonzalez-Hernandez, S.S.Chao, S.C.Lee and K.Tanaka, *Appl.Phys.Lett.* **40** 534 (1982).

[9] Z.Iqbal and S.Veprek, *J.Phys.C:Solid State Phys.,* **15** 377 (1982)